Computational Study on the Attack of . OH Radicals on Aromatic Amino Acids

ARTICLE *in* CHEMISTRY - A EUROPEAN JOURNAL · MAY 2013

Impact Factor: 5.73 · DOI: 10.1002/chem.201203862 · Source: PubMed

3 AUTHORS, INCLUDING:

Jon I Mujika
Universidad del País Vasco / Euskal Herriko…
31 PUBLICATIONS **390** CITATIONS
SEE PROFILE

Jon M Matxain
Universidad del País Vasco / Euskal Herriko…
83 PUBLICATIONS **1,422** CITATIONS
SEE PROFILE

CHEMISTRY
A EUROPEAN JOURNAL

ChemPubSoc
Europe

DOI: 10.1002/chem.201203862

Computational Study on the Attack of ·OH Radicals on Aromatic Amino Acids

J. I. Mujika,* J. Uranga, and J. M. Matxain[a]

Abstract: The attack of hydroxyl radicals on aromatic amino acid side chains, namely phenylalanine, tyrosine, and tryptophan, have been studied by using density functional theory. Two reaction mechanisms were considered: 1) Addition reactions onto the aromatic ring atoms and 2) hydrogen abstraction from all of the possible atoms on the side chains. The thermodynamics and kinetics of the attack of a maximum of two hydroxyl radicals were studied, considering the effect of different protein environments at two different dielectric values (4 and 80). The obtained theoretical results explain how the radical attacks take place and provide new insight into the reasons for the experimentally observed preferential mechanism. These results indicate that, even though the attack of the first ·OH radical on an aliphatic C atom is energetically favored, the larger delocalization and concomitant stabilization that are obtained by attack on the aromatic side chain prevail. Thus, the obtained theoretical results are in agreement with the experimental evidence that the aromatic side chain is the main target for radical attack and show that the first ·OH radical is added onto the aromatic ring, whereas a second radical abstracts a hydrogen atom from the same position to obtain the oxidized product. Moreover, the results indicate that the reaction can be favored in the buried region of the protein.

Keywords: amino acids · density functional calculations · oxidation · radicals · reaction mechanisms

1. Introduction

Free radicals are highly reactive chemical species that contain unpaired electrons. Depending on their nature, they are classified as reactive oxygen (ROS), nitrogen (RNS), carbon (RCS), or sulfur species (RSS). These radicals are necessary intermediates in many biochemical processes and they are involved in many reactions that constitute the typical biological activity of organisms. Nevertheless, excess radical species can produce severe damage in an organism, if the correct balance between their production and annihilation is uncontrolled.[1,2] Three type of molecules are responsible for controlling the overproduction of radicals in an organism: 1) Enzymes, such as superoxide dismutase (SOD), catalase (CAT), glutathione peroxidase (GSHPx), and glutathione reductase (GSSGR); 2) low-molecular-weight antioxidants, such as glutathione; and 3) vitamins. However, molecular dysfunction may cause the overproduction of these reactive species, thus affecting a large number of tissues in the organism. Such an excess of radical species, especially ROS, has been related to various diseases, such as ischemia/reperfusion, atherosclerosis, and diabetes mellitus, or to neurodegenerative diseases, such as Parkinson's and Alzheimer's diseases.[3] In fact, it has been measured that the formation of free radicals in patients with Alzheimer's disease was 22% higher than in normal control subjects.[4] Therefore, it is believed that an excess of ROS species, also known as "oxidative stress", plays a crucial role in the development of this disease[5,6] because these species alter and damage the structure and function of membrane lipids, DNA and RNA nucleic acids, and proteins.

In terms of proteins and enzymes, the main target of ROS can either be the protein backbone or the side chains on the amino acids, in both cases causing the loss of biological activity of the macromolecule.[7–9] Concretely, in the case of aliphatic amino acids, Stadtman[10] determined by using radiolysis that, for simple aliphatic amino acids, the most common pathway involves the abstraction of a hydrogen atom from the alpha carbon atom of an amino acid residue. In contrast, for larger aliphatic amino acids, hydrogen abstraction from other positions on the side chain of the residue becomes more important and leads to the formation of either hydroxy derivatives or amino acid cross-linked products as a consequence of carbon-centered radical-recombination processes.[10] On the other hand, hydrogen abstraction plays a minor role in the oxidation of aromatic amino acids and, instead, the aromatic ring is the primary site for the addition of the radical to form hydroxy derivatives, which leads to ring scission or, in the case of tyrosine, to the formation of Tyr–Tyr cross-linked dimers.

The attack of ROS species onto the three aromatic amino acid side chains, namely phenylalanine, tyrosine, and tryptophan, gives rise to well-defined products (Figure 1 A). When

[a] Dr. J. I. Mujika, J. Uranga, Dr. J. M. Matxain
Kimika Fakultatea, Euskal Herriko Unibertsitatea (UPV/EHU)
and Donostia International Physics Center
PK 1072, 20080 Donostia, Euskadi (Spain)
Fax: (+34) 943015270
E-mail: joni.mujika@ehu.es

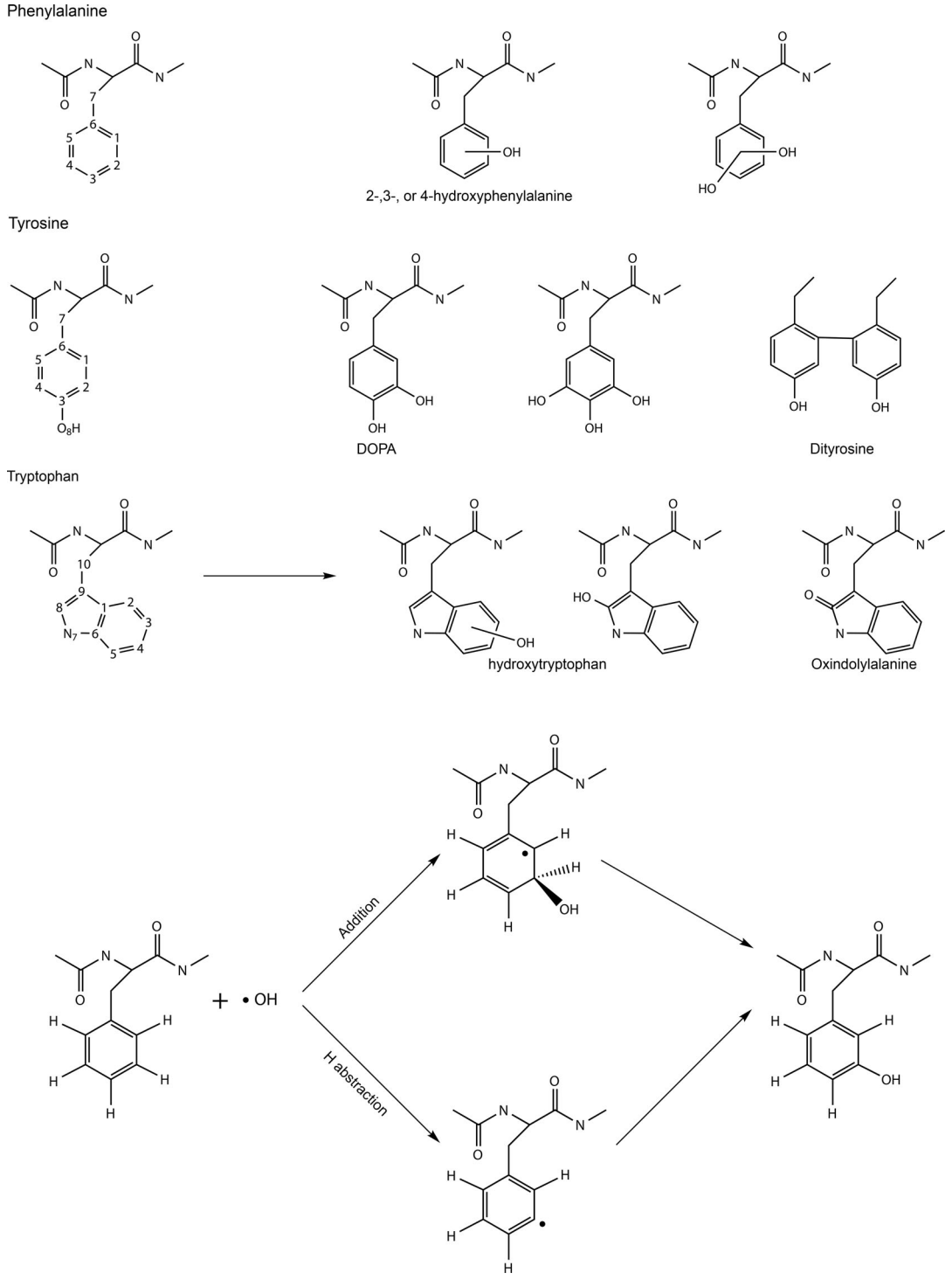

Figure 1. Top: Atom labeling of the three aromatic amino acids that were studied, that is, phenylalanine, tyrosine, and tryptophan; the experimentally characterized hydroxylation products are also shown. Bottom: The two reaction mechanisms that were considered in this work, that is, ˙OH addition and hydrogen abstraction.

an ˙OH radical, one of the most reactive species, attacks the phenylalanine side chain, the main reaction is the oxidation of the aromatic ring to form different isomers of tyrosine (Figure 1 A).[11] The final product depends on the position on the ring that the ROS species attacks and, thus, *para*-, *ortho*-, or *meta*-tyrosine may be produced. *para*-Tyrosine, or L-tyrosine, is found in nature, whereas the other two isomers are rare and arise from the non-enzymatic free-radical hydroxylation of phenylalanine under the conditions of oxidative stress.[12] *meta*-Tyrosine and its analogues have been syn-

thesized in the laboratory and they have shown applications in Parkinson's disease, Alzheimer's disease, and arthritis.[13] On the other hand, Li et al.[14] combined laser-induced acoustic desorption (LIAD) with Fourier transform ion cyclotron resonance mass spectrometry (FT-ICR) to study the damage that phenyl radicals may cause in neutral dipeptides in the gas phase. This study concluded that the phenyl radical may abstract a hydrogen atom from all of the studied dipeptides, with the SCH_3 side chain of cysteine the preferred target.

Tyrosine radicals can either be found in reactions that are catalyzed by enzymes as intermediates[15] or are produced from tyrosyl peptides through the action of peroxidases.[16] The attack of a hydroxyl radical onto a tyrosine moiety produces two isomers, 2,3- and 3,4-dihydroxyphenylalanine, known as DOPA (Figure 1 A).[11] DOPA has been used as a drug in the treatment of Parkinson's disease.[17] In addition, two tyrosyl radicals can combine to form a bi-tyrosine species.[18,19]

Tryptophan contains two rings in its side chain and, therefore, it is more exposed to the attack of ROS species.[20] When the OH radical attacks the aromatic ring, several hydroxyl derivatives are formed, whereas, when the pyrrole ring is the target of the attack, oxindolylalanine, *N*-formylkynurenine, or kynurenine are the main products.[8,21] In this sense, a deep knowledge of the tryptophan oxidative radical intermediate is of relevant importance, because intramolecular and intermolecular electron transfer between a tyrosine moiety and an oxidized tryptophan radical is a relevant process in biological systems.[22,23]

Experimentally, it is difficult to trap radical species, owing to their short half times. In this sense, computational chemistry can provide valuable information for characterizing entire reaction pathways, as different investigations have demonstrated.[24–32] Herein, we report the alternative reaction pathways in the sequential attack of two $^{\bullet}OH$ radicals onto phenylalanine, tyrosine, and tryptophan amino acid side chains, all of which are characterized within the framework of density functional theory. Two type of reactions have been considered (Figure 1 B), that is, hydrogen abstraction by the radical and the addition of this species onto the aromatic rings of the amino acid side chains. The attack of $^{\bullet}OH$ radicals on all of the possible positions in the amino acid side chains was considered. The obtained results provide valuable data in elucidating the most favored oxidized products, both thermodynamically and kinetically, along with the favored mechanisms of these reactions.

2. Methods and Models

This study was carried out by using the Gaussian 09 package[33] with the meta-GGA functional MPWB1K, as developed by Truhlar and co-workers,[34–37] within density functional theory.[38,39] Structure optimizations were performed in the gas phase by using the 6-31+G(d,p) basis set. Harmonic vibrational frequencies were obtained by analytical differentiation of the gradients to determine whether the structures were minima or transition states and to evaluate the zero-point vibrational energy (ZPVE), the thermal (298 K) corrections to the enthalpy, and the Gibbs free energy in the harmonic oscillator approximation. Single-point calculations were performed by using the 6-311++G-(2df,2p) basis set and the integral equation formalism of the polarized continuum model (IEFPCM) of Tomasi and co-workers[40,41] on the optimized structures to estimate the effects of bulk solvent. Two dielectric constants were employed in these calculations: 1) $\varepsilon=4$, to consider a low solvent-accessible area inside a protein and 2) $\varepsilon=80$ in bulk aqueous solution. It should be noted that the reactions studied in this work considered infinitely separated reactants and products, which led to an overestimation of the entropic effects and, therefore, the enthalpy values (ΔH^{298}) were considered for discussion purposes. These values were determined by adding the enthalpic contributions in the gas phase to the electronic energies in solution to give the final enthalpies, ΔH_4^{298} and ΔH_{aq}^{298}. It has been demonstrated elsewhere that this method is appropriate for studying these types of reactions.[24,42,43] In addition, to test the reliability of this method, the energies of two set of reactions were compared with the available experimental data, that is: 1) bond-dissociation energies and 2) hydrogen abstraction from small molecules. These values are presented in Table 1. Overall, an encouraging agreement between the computed and experimental data is observed, with a mean absolute deviation (MAD) of about 2 kcal mol^{-1}.

Table 1. Comparison between the computed (see Methods and Models section) and experimental energies (in kcal mol^{-1}) for two types of radical reactions, that is, bond dissociation and hydrogen abstraction from small molecules.

Reaction	Computed	Experimental	Difference
Bond dissociation			
$CH_4 \rightarrow CH_3^{\bullet} + {}^{\bullet}H$	112.4	113.0	−0.6
$NH_3 \rightarrow NH_2^{\bullet} + {}^{\bullet}H$	114.2	115.9	−1.7
$H_2O \rightarrow {}^{\bullet}OH + {}^{\bullet}H$	122.3	126.0	−3.7
$C_2H_6 \rightarrow C_2H_5^{\bullet} + {}^{\bullet}H$	107.9	109.4	−1.5
$H_2O_2 \rightarrow HOO^{\bullet} + {}^{\bullet}H$	89.1	92.7	−3.6
$C_2H_6 \rightarrow 2\,CH_3^{\bullet}$	98.7	96.6	2.1
$H_2O_2 \rightarrow 2\,{}^{\bullet}OH$	49.4	55.0	−5.6
MAD			−2.1
H abstraction			
$CH_4 + {}^{\bullet}OH \rightarrow CH_3^{\bullet} + H_2O$	−9.9	−13.0	3.1
$NH_3 + {}^{\bullet}OH \rightarrow NH_2^{\bullet} + H_2O$	−8.2	−10.1	1.9
$C_2H_6 + {}^{\bullet}OH \rightarrow C_2H_5^{\bullet} + H_2O$	−14.4	−16.6	2.2
$H_2O_2 + {}^{\bullet}OH \rightarrow HOO^{\bullet} + H_2O$	−33.3	−33.3	0.0
MAD			1.8

The model structures of the three studied aromatic amino acids (Figure 1 A) show two peptide bonds that flank the side chain of the amino acid. The dihedral angles are oriented to simulate a beta sheet. The protein chain is expected to very slightly alter the kinetics and thermodynamics of the studied reactions. Nevertheless, one should bear in mind that the steric effects could be different for other types of

protein folding. The N and O terminals of these two peptide bonds are capped by a methyl group, thus simulating the C_α atom of the lateral amino acids. As a consequence, the two faces of the aromatic ring are not completely symmetric (for example, see Figure 2). Hence, the attack of a radical onto the aromatic ring is not equivalent from both sides of the ring and, overall, the approximation of the radical from the N-terminal face leads to more-stable products. Therefore, for consistency, only the attacks from this side are considered herein.

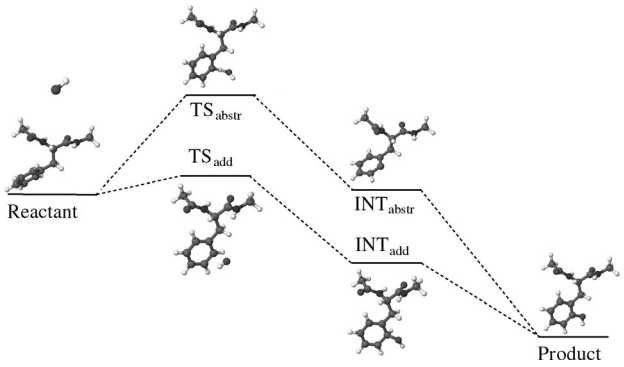

Figure 2. Stationary points along the characterized reaction pathways for the attack of two •OH radicals on the C1 atom of phenylalanine, following addition and hydrogen-abstraction mechanisms; the energy levels are not to scale.

3. Results

The attack of an •OH radical onto three aromatic amino acid side chains, that is, the side chains of phenylalanine, tyrosine, and tryptophan, is investigated. The characterized reaction pathway includes the sequential attack of two •OH radicals, thus implying the formation of a radical intermediate. Two type of reactions have been considered: 1) The addition of •OH radicals to the aromatic ring, with the formation of radical adducts, and 2) H abstraction, in which a hydrogen atom is abstracted from all of the possible side-chain atoms by a radical to yield a radical intermediate and a water molecule (Figure 1 B). In both cases, the transition states, which determine the kinetics of the reactions, and intermediates were characterized. Then, the attack of a second radical onto the radical intermediate was analyzed. Because this step involves the reaction between two radical species, no stable transition state is expected and, therefore, only the final products are characterized. Thus, the kinetics of the reactions are determined by the energy barrier of the first step. The final products are the result of the sequential attack of two hydroxyl radicals onto the amino acid by abstraction and addition reactions, regardless of the order in which they take place. Therefore, the entire reaction pathway can be considered as the substitution of a hydrogen atom by a hydroxyl group and it can only take place at C atoms with at least one hydrogen atom. This reaction pathway implies that the concentration of •OH radicals is high enough to allow the rapid attack of the second •OH radical onto the radical intermediate. We should bear in mind that, in biological systems, the aromatic amino acid (or the radical intermediate) might be exposed not only to •OH radicals but also to a large range of other radical species. Thus, many other reaction mechanisms may also occur. However, the simplest reaction pathway that can explain the formation of many of the experimentally characterized oxidized products is the sequential attack of two •OH radicals and, consequently, this pathway has been characterized in this study.

3.1. Phenylalanine: The reaction pathways for the attack of two •OH radicals onto the side chain of phenylalanine are described in this subsection. As mention above, two reaction mechanisms have been considered: 1) Addition to the double-bonded ring carbon atoms and 2) hydrogen abstraction. The entire process involves a two-step pathway in which the two mechanisms are combined sequentially, that is, addition/abstraction or abstraction/addition.

Attack of a first •OH radical. The addition of an •OH radical onto each of the six C atoms that comprise the aromatic ring and the hydrogen abstraction from each of the seven C atoms of the side chain (atoms of the aromatic ring and the C_β atom, C7 in Figure 1 A) have been calculated. The main geometric parameters, the spin densities on the radical O atom and the attacked C atom, and the enthalpies of all of these reaction mechanisms at two different dielectrics (4 and aq) are given in Table 2. As an example, the optimized stationary points in the attack of •OH radicals, both for addition and abstraction, onto the C1 atom are shown in Figure 2.

The enthalpy barriers to all of the addition reactions are very low and, in some cases, show negative values. Notably, these values are calculated compared to the infinitively separated reactants, but the reaction first proceeds through a reactant complex between phenylalanine and an •OH radical. However, considering all of the reaction mechanisms that are involved, a large number of reactant complexes and products are expected to form, without significantly altering the conclusions of this work. As an example, we characterized one of the possible reactant complexes (not necessarily the most stable one) that was formed between phenylalanine and the hydroxyl radical (Figure 2 and Table 2), which was energetically slightly below all of the transition states. In five of the six addition-reaction pathways, the enthalpy barriers were in the range -1.0 to $1.0\,kcal\,mol^{-1}$ with $\varepsilon=4$ and in the range 1–2 $kcal\,mol^{-1}$ with $\varepsilon=80$. The exception was addition on the C5 atom, because the hydrogen-bond interaction between the oxygen atom of the hydroxyl radical and the proton of an amide group decreased the ΔH_4^{298} and ΔH_{aq}^{298} values to -4.5 and $-1.3\,kcal\,mol^{-1}$, respectively. On the other hand, the energy barriers for H abstraction from the aromatic ring atoms were significantly larger, with

Table 2. Computed enthalpy values (in kcal mol^{-1}) at dielectric constants of 4 and 80 (in aqueous solution) of the transition states and radical intermediates for the attack of the first $^{\bullet}$OH radical onto phenylalanine, considering two reaction mechanisms, that is, addition and abstraction. The C–O distance (addition) and the C–H and O–H distances (abstraction) are also shown (in Å). The spin densities on the radical O atoms (ρ_s^O) and target C atoms (ρ_s^C) are also presented, as well as the data of one of the reactant complexes.

Phe–$^{\bullet}$OH complex

	r_{CO}	ΔH_4	ΔH_{aq}	ρ_s^O	ρ_s^C
	2.614	−4.8	−1.7	0.93	0.02

$^{\bullet}$OH addition

	r_{CO}^{TS}	ΔH_4^{TS}	ΔH_{aq}^{TS}	ρ_s^O	ρ_s^C	r_{CO}^{Int}	ΔH_4^{Int}	ΔH_{aq}^{Int}	ρ_s^O	ρ_s^C
C1	1.985	−0.4	1.1	0.65	−0.15	1.425	−18.0	−17.2	0.02	−0.16
C2	1.969	1.0	1.7	0.65	−0.16	1.423	−16.3	−16.0	0.02	−0.15
C3	1.974	0.4	1.0	0.65	−0.15	1.423	−18.0	−17.0	0.02	−0.09
C4	1.965	1.0	1.7	0.64	−0.17	1.419	−16.5	−15.5	0.02	−0.18
C5	2.011	−4.5	−1.3	0.62	−0.13	1.434	−17.7	−15.1	0.02	−0.23
C6	1.999	−0.5	0.6	0.64	−0.11	1.442	−18.6	−14.9	−0.03	−0.09

H abstraction

	r_{CH}^{TS}	r_{OH}^{TS}	ΔH_4^{TS}	ΔH_{aq}^{TS}	ρ_s^O	ρ_s^C	ΔH_4^{Int}	ΔH_{aq}^{Int}
C1	1.236	1.240	4.1	4.9	0.58	0.41	−4.6	−4.9
C2	1.241	1.228	3.7	4.1	0.58	0.42	−4.7	−5.5
C3	1.240	1.229	4.1	4.7	0.58	0.42	−4.2	−4.9
C4	1.248	1.219	5.3	6.7	0.57	0.48	−5.4	−6.2
C5	1.259	1.208	2.2	5.4	0.56	0.46	−4.9	−5.4
C7	1.149	1.524	0.1	3.2	0.78	0.32	−29.7	−29.1

values in the range 3.7–5.3 kcal mol^{-1} for ΔH_4^{298} and 4.1–6.7 kcal mol^{-1} for ΔH_{aq}^{298}. Clearly, the attack of a radical onto the aromatic ring atoms favors the formation of the adduct intermediates, as could be expected. However, the energy barrier for H abstraction from the aliphatic C7 atom is similar to those of addition reactions. Therefore, from a kinetics point of view, the addition to the aromatic ring and H abstraction from the C7 atom are competitive processes. However, thermodynamically, the abstraction from the C7 atom is clearly favored. The values of ΔH_4^{298} and ΔH_{aq}^{298} are close to −29 kcal mol^{-1}, about 14 kcal mol^{-1} more stable than the intermediates that are formed by the addition of the hydroxyl radical.

Next, we focused on the geometric parameters of these reactions. In the addition reactions, the $^{\bullet}$OH radical approached the attacked C atom perpendicular to the aromatic ring, thereby resulting in a similar O_{OH}–C distance in all of the characterized transition states (in the range 1.97–2.01 Å). The longest distance was observed in the transition state that corresponded to the attack on the C5 carbon atom (2.011 Å), owing to a hydrogen-bond interaction between the O_{OH} atom and the H_{NH} atom on the backbone (O_{OH}–HN, 1.913 Å). Once the attack takes place, a radical intermediate is formed. The O_{OH}–C distances are similar in all of the characterized intermediates, within the range 1.42–1.44 Å. Again, the proximity of the backbone determines the length of this distance and the hydrogen-bond interaction between the O_{OH} and H_{NH} atoms lengthens the O_{OH}–C distance to 1.434 and 1.442 Å in Int_{Phe}^{C5add} and Int_{Phe}^{C6add}, respectively. In the abstraction reaction from the aromatic ring, the hydroxyl radical approaches in the same plane as the ring, thus leading to very similar geometric features in all of the characterized reaction pathways. In the transition state, the finally abstracted hydrogen is shared by the hydroxyl O atom and the ring C atom, both with distances of about 1.2 Å. However, for the hydrogen abstraction from the aliphatic C7 atom, the transition state occurs during an earlier stage, because the hydrogen atom is closer to the C atom (1.149 Å) than to the oxygen atom (1.524 Å). This result is in agreement with the smaller calculated reaction barriers.

Finally, we analyzed the spin density on the O_{OH} atom (ρ_s^O) and on the target C atom (ρ_s^C), which indicated the evolution of the location of the radical character along the reaction coordinates. In the case of the addition reactions, the trend was similar for all of the aromatic carbon atoms. For infinitely separated atoms, the radical character was fully localized on the O atom of the hydroxyl radical; then, in the TS structures, ρ_s^O decreased to about 0.65. Note that $\rho_s^C \approx -0.15$, which denotes a delocalization of the remaining radical character (about −0.20) along the aromatic ring. In the adducts, the radical character is fully delocalized over the aromatic ring, as one may deduce from the values of about 0.02 and −0.15 for ρ_s^O and ρ_s^C, respectively. The behavior of the spin density is different for the H-abstraction reaction.

For the abstraction from the aromatic ring, the radical character is roughly 60% on the O atom and 40% on the C atom. Hence, the radical character is completely localized on the O_{OH} and attacked C atoms. On the other hand, the radical character on the O_{OH} atom grows to 78% during the attack on the aliphatic C7 atom, which is in agreement with the fact that there is an earlier TS in this case and, as a consequence, less radical character is transferred onto the C7 atom.

Attack of a second $^{\bullet}$OH radical. Owing to its high reactivity, the radical intermediate that is formed after the reaction of phenylalanine with a first hydroxyl radical is prompted to react with a second hydroxyl radical to form a non-radical product. As was pointed out above, this reaction can only take place at C atoms that contain at least one hydrogen atom. This fact reduces the possibilities to five C atoms in the aromatic ring, as well as the C7 atom. In addition, note that H abstraction from the C_α atom would lead to the formation of a double bond between the carbon atoms that are close to the aromatic ring. This process could be thermodynamically favored, owing to the formation of an extra conjugated double bond near to the aromatic ring. Therefore, in this special case, abstraction from the backbone was considered. The reaction enthalpies of all of these products are listed in Table 3.

The oxidation of C atoms that are located on the aromatic ring is a very favorable reaction. The enthalpy values are very similar for the five products, with ΔH_{aq}^{298} values in the

Table 3. Computed enthalpy values (in kcal mol^{-1}) at dielectric constants of 4 and 80 (in aqueous solution) calculated with respect to the initial reactants and products that are formed by the attack of a second hydroxyl radical onto phenylalanine.

	ΔH_4^{298}	ΔH_{aq}^{298}
$Prod_{Phe}^{C1}$	−117.1	−116.6
$Prod_{Phe}^{C2}$	−116.9	−116.7
$Prod_{Phe}^{C3}$	−116.5	−116.2
$Prod_{Phe}^{C4}$	−116.4	−115.1
$Prod_{Phe}^{C5}$	−115.9	−114.5
$Prod_{Phe}^{C7}$	−111.0	−108.4
$Prod_{Phe}^{C7\alpha}$	−102.5	−100.6

range −114 to −117 kcal mol^{-1}; in all cases, the ΔH_4^{298} values are very similar. In spite of the small differences between them, a deeper analysis of the ΔH_{aq}^{298} values indicate that the oxidation reaction at the C1 and C2 atoms shows the most favorable enthalpies ($\Delta H_{aq}^{298} = -117$ kcal mol^{-1}), followed by a value of −116 kcal mol^{-1} when the oxidation take place at the C3 atom; at the C4 and C5 atoms, the values are −115 and −114 kcal mol^{-1}, respectively. These values suggest that there is not any preference in terms of the ring position and that the attack of the hydroxyl radical is equally likely at *ortho*-, *meta*-, or *para* positions; instead, the position of the ring with respect to the backbone may influence the final stability of the product, without considering steric effects.

Departing from the radical intermediate that is formed by the abstraction of a hydrogen atom from the aliphatic C7 carbon atom (Int_{Phe}^{C7ab}), two alternative products can be formed: 1) The addition of a second hydroxyl group onto the C7 atom ($Prod_{Phe}^{C7}$) or 2) abstraction of the hydrogen atom from the C_α atom ($Prod_{Phe}^{C7\alpha}$). The ΔH_{aq}^{298} values for these stationary points show that $Prod_{Phe}^{C7}$ is more stable, with a value of −108.4 kcal mol^{-1}. However, even though Int_{Phe}^{C7ab} is clearly the most stable radical intermediate, the oxidation at the C7 position is about 8 kcal mol^{-1} less stable than that at any of the aromatic C atoms. Therefore, if the concentration of the radical is high enough to allow two hydroxyl molecules to reach the phenylalanine side chain, the oxidation of any of the aromatic ring atoms would be the most favored products for to thermodynamic, kinetic, and steric reasons.

3.2. Tyrosine: In this subsection, we describe the reaction pathways for the attack by two •OH radicals on the double-bonded ring carbon atoms and hydrogen abstraction from all of the possible atoms on the amino acid side chain of tyrosine. In the first step, both the addition and abstraction reactions were considered, whereas, for the second step, only individual addition or abstraction processes were considered, depending on the first step.

Attack of a first •OH radical. The difference between phenylalanine and tyrosine side chains is a hydroxy group at the *para* position in the aromatic ring, on the C3 atom. Therefore, the studied addition reactions of tyrosine are similar to previously studied processes in phenylalanine, but H abstraction now takes place from the O8 atom instead of from the C3 atom. The main geometric parameters, spin densities on the radical O atom and on the target atom, and the enthalpies of all of these reaction mechanisms at two different dielectrics (4 and aq) are listed in Table 4. The optimized stationary points are not given for the sake of brevity, because they resemble those of phenylalanine.

The potential-energy surfaces for the addition of the first hydroxyl radical onto the aromatic C atoms of tyrosine resemble those computed for phenylalanine. Therefore, the hydroxy group in tyrosine has little effect on the addition of the hydroxyl radical. The calculated energy barriers ΔH_4^{298} (−3.4 to 2.5 kcal mol^{-1}) and ΔH_{aq}^{298} (−1.1 to −4.3 kcal mol^{-1}) are similar to those obtained for phenylalanine, although with larger differences. The highest barrier in the radical attack onto the C3 atom may be due to the influence of the hydroxy group that is located on this atom. On the other hand, attack on the C5 and C6 atoms shows the lowest barriers, owing to the influence of the backbone. The enthalpies of the radical intermediate adducts are close to one another, as was the case for phenylalanine. At $\varepsilon = 4$, the most stable structure is Int_{Tyr}^{C6}, with a value of −19.5 kcal mol^{-1}, and Int_{Tyr}^{C1} is the least stable one, with a relative enthalpy of −16.7 kcal mol^{-1}. On the other hand, in aqueous solution, Int_{Tyr}^{C3} is the most stable intermediate, with a ΔH_{aq}^{298} value of −17.8 kcal mol^{-1}, and Int_{Tyr}^{C1} is the least stable one, with a value of −14.4 kcal mol^{-1}.

Table 4. Computed enthalpy values (in kcal mol^{-1}) at dielectric constants of 4 and 80 (in aqueous solution) at the transition states and radical intermediates for the attack of the first •OH radical onto tyrosine, considering two reaction mechanisms, that is, addition and abstraction. The C–O distance (addition) and the C–H and O–H distances (abstraction) are also shown (in Å). The spin densities on the radical O atoms (ρ_s^O) and target C atoms (ρ_s^C) are also presented, as well as the data of one of the reactant complexes.

Tyr–•OH complex

	r_{CO}	ΔH_4	ΔH_{aq}	ρ_s^O	ρ_s^C
	2.587	−4.3	−1.2	0.92	0.00

OH addition

	r_{CO}^{TS}	ΔH_4^{TS}	ΔH_{aq}^{TS}	ρ_s^O	ρ_s^C	r_{CO}^{Int}	ΔH_4^{Int}	ΔH_{aq}^{Int}	ρ_s^O	ρ_s^C
C1	1.981	0.9	2.3	0.64	−0.17	1.426	−16.7	−15.7	0.02	−0.13
C2	1.996	0.6	0.8	0.66	−0.11	1.418	−18.1	−17.2	0.02	−0.09
C3	2.005	2.5	4.3	0.63	-0.12	1.420	−18.9	−17.8	0.03	−0.10
C4	2.000	1.1	3.2	0.57	−0.04	1.425	−18.2	−15.9	0.01	−0.27
C5	2.036	−3.4	−0.3	0.62	−0.12	1.438	−17.0	−14.4	0.02	−0.19
C6	2.034	−1.8	−1.1	0.64	−0.11	1.446	−19.5	−15.9	0.02	−0.09

H abstraction

	r_{CH}^{TS}	r_{OH}^{TS}	ΔH_4^{TS}	ΔH_{aq}^{TS}	ρ_s^O	ρ_s^C	ΔH_4^{Int}	ΔH_{aq}^{Int}
C1	1.236	1.239	5.2	5.9	0.59	0.39	−3.7	−3.6
C2	1.264	1.194	6.2	6.9	0.57	0.35	−2.2	−2.6
C4	1.245	1.236	5.8	8.8	0.54	0.38	−2.6	−2.5
C5	1.260	1.205	3.0	6.2	0.56	0.46	−3.8	−4.2
C7	1.141	1.575	0.9	4.1	0.79	0.29	−29.6	−29.1
O8	0.988	1.456	2.4	4.8	0.68	0.20	−29.3	−28.8

As was the case with phenylalanine, the energy barriers for hydrogen abstraction from the aromatic ring are slightly larger than for the addition reactions, with enthalpy barriers of about 6–7 kcal mol^{-1}. Thermodynamically, these processes are also less favorable. However, H abstraction from the C7 and O8 atoms show similar energy barriers as the addition processes, but, thermodynamically, both processes are favored by about 12 kcal mol^{-1}. Sterically, abstraction from the O8 atom would be favorable compared to from the C7 atom and, therefore, these results suggest that the attack of a first hydroxyl radical would eventually abstract a hydrogen atom from the O8 position, rather than other abstraction or addition processes. In this case, the hydroxyl O atom approaches to 1.456 Å from the abstracted H, whereas the O8–H distance is very slightly elongated to 0.988 Å. This early TS geometry is in agreement with the small calculated barrier. Notably, the spin density that is located on the hydroxyl O atom is larger than in the abstractions from the aromatic carbon atoms. The geometric and spin-density analysis for the remaining cases are very similar to those of phenylalanine.

Attack of a second ·OH radical. The radical intermediate that is formed from the reaction of tyrosine with a first hydroxyl radical is prompted to react with a second hydroxyl radical to form a non-radical product. The reaction enthalpies of all of the characterized products are listed in Table 5.

Table 5. Computed enthalpy values (in kcal mol^{-1}) at dielectric constants of 4 and 80 (in aqueous solution) calculated with respect to the initial reactants and products that are formed by the attack of a second hydroxyl radical onto tyrosine.

	ΔH_4^{298}	ΔH_{aq}^{298}
$Prod_{Tyr}^{C1}$	−116.5	−115.9
$Prod_{Tyr}^{C2}$	−114.9	−113.4
$Prod_{Tyr}^{C4}$	−114.1	−111.6
$Prod_{Tyr}^{C5}$	−116.4	−113.6
$Prod_{Tyr}^{C7}$	−111.0	−108.5
$Prod_{Tyr}^{C7\alpha}$	−101.3	−99.6
$Prod_{Tyr-Tyr}^{OO}$	−37.3	−30.9
$Prod_{Tyr-Tyr}^{22}$	−107.7	−104.5

As in phenylalanine, the attack of a second radical onto the aromatic carbon atoms produces very stable oxidized products. The ΔH_{aq}^{298} values of the four possible oxidized products (in the *ortho*- and *meta* positions) are within the range −111 to −116 kcal mol^{-1}. Among these products, the most stable product corresponds to oxidation at the C1 atom, with ΔH_4^{298} and ΔH_{aq}^{298} values of about −116 kcal mol^{-1}. These thermodynamics data do not explain the experimental formation of 2,3- and 3,4-dihydroxyphenylalanine (DOPA) rather than 1,3 or 3,5-dihydroxyphenylalanine. Even though the difference in the enthalpy values is small, the formation of the final DOPA products is driven by factors other than thermodynamics (see the Discussion section).

The most stable radical intermediates were formed by hydrogen abstraction from the C7 and O8 atoms. From Int_{Tyr}^{C7ab}, two alternative products were considered: 1) The addition of the radical to afford the oxidized product ($Prod_{Tyr}^{C7}$) and 2) a second abstraction from C_α to form a double bond between this atom and the C7 atom. Addition at the C7 atom shows a $\Delta H_{aq}^{298} = -108.5$ kcal mol^{-1}, which is about 3–5 kcal mol^{-1} less stable than the attack onto an aromatic C atom; the abstraction from C_α is less favorable, with an enthalpy of −99.6 kcal mol^{-1}. Therefore, as with phenylalanine, these two reactions are less favorable than the oxidation reaction on the aromatic ring.

Finally, the exposure of tyrosine to radicals may produce some bi-tyrosine cross-linked species (Figure 1 A), which are formed from the reaction between two tyrosine radical intermediates. Herein, two bi-tyrosine molecules, from intermediates Int_{Tyr}^{C2} or Int_{Tyr}^{O8} (Figure 3), were characterized, that is, the products of cross-linking through the C2 and O8 atoms, respectively. The enthalpy values are negative for both bi-tyrosine species and the species that is cross-linked through the C2 atoms is much more stable than that through the O8 atoms, as they show ΔH_{aq}^{298} values of −104.5 and

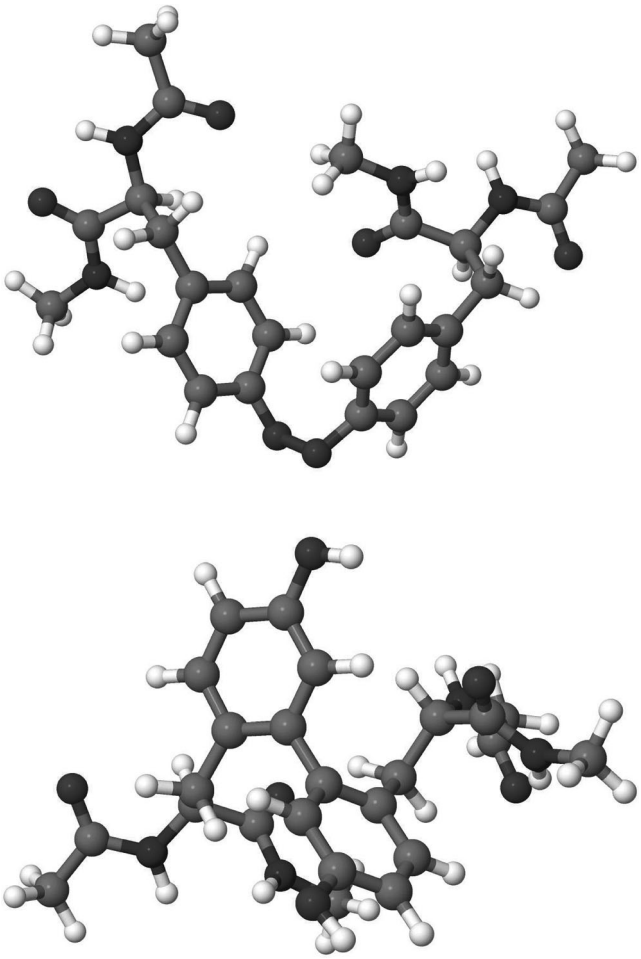

Figure 3. Two characterized cross-linked bi-tyrosine products, which are linked through the O8 (top) and C2 atoms (bottom).

−30.9 kcal mol^{-1}, respectively. These results are in agreement with the experimentally characterized bi-tyrosine species, which were linked through aromatic C atoms. However, the reaction is thermodynamically less favorable than the oxidation reaction, which may suggest that the bi-tyrosine species are formed owing to other factors (see the Discussion section).

3.3. Tryptophan: The side chain of tryptophan differs significantly from those of phenylalanine and tyrosine, because it is composed of a bicyclic indole group with six-membered and five-membered rings. The exposure of tryptophan to •OH radicals leads to several products, according to experimental evidence (Figure 1 A). Reaction pathways for the attack of two •OH radicals on the double-bonded ring atoms of tryptophan are studied in this subsection. Note that, for H abstraction, the C_β (C10) atom has also been considered, as for phenylalanine and tyrosine.

Attack of a first •OH radical. Five addition reactions on the two tryptophan rings have been characterized, namely at the C2, C3, C4, C5, and C8 atoms. Notably, the addition of the radical onto the N7 atom does not lead to a stable stationary point, owing to fact that it is not doubly bonded to any neighboring atoms. The considered H abstractions are from the above-mentioned C atoms, as well as from the N7 and C10 atoms. The main geometric parameters, spin densities on the radical O atom and on the target atom, and the enthalpies of all these reaction mechanisms at two different dielectrics (4 and aq) are listed in Table 6.

The enthalpy barriers of the addition processes are small, as in the previous cases with phenylalanine and tyrosine. Addition at the C8 position is the most favorable, as indicated by the ΔH_4^{TS} and ΔH_{aq}^{TS} values of −5.7 and −4.8 kcal mol^{-1}, respectively. According to the enthalpies of intermediate radical formation, Int_{Trp}^{C8ad} is also the most stable intermediate, with a ΔH_{aq}^{TS} value of −27.4 kcal mol^{-1}, followed by Int_{Trp}^{C2ad} (−21.2 kcal mol^{-1}); the ΔH_{aq}^{TS} of the remaining intermediates are in the range −15 to 19 kcal mol^{-1}. Therefore, the computed enthalpies for the attacks on atoms C2–C5 are comparable to the attacks on the aromatic rings of phenylalanine and tyrosine, but the enthalpy of Int_{Trp}^{C8ad} is about 10 kcal mol^{-1} more stable and that of Int_{Trp}^{C2ad} is about 5 kcal mol^{-1} more stable. These results show that the addition of the first •OH radical to these atoms is the most favored addition process with all of the aromatic amino acid side chains.

Next, we focused on the calculated enthalpies for the H-abstraction processes. According to enthalpy barriers and enthalpies of intermediate formation, two separated cases can be clearly distinguished: On the one hand, H abstraction from the C atoms of the six-membered ring show enthalpy barriers of about 5 kcal mol^{-1}. The ΔH_{aq}^{Int} values of the intermediates are between −3 and −4 kcal mol^{-1} and, hence, about 10 kcal mol^{-1} less stable than radical addition at the same C atoms.

On the other hand, the most reactive positions for the H abstraction are the N7 atom in the five-membered aromatic ring and the C10 position (as in tyrosine and phenylalanine). The enthalpy barriers for the abstractions from these two atoms are competitive with those of the addition processes, but, more importantly, the ΔH_{aq}^{Int} values of the intermediates are −24.6 for Int_{Trp}^{N7ab} and −27.7 kcal mol^{-1} for Int_{Trp}^{C10ad}. Finally, all attempts to characterize the transition state for abstraction from the C8 position failed, apparently owing to the influence of the backbone. Nevertheless, the ΔH_{aq}^{Int} value for the C8 atom is the only endothermic process and, therefore, the energy barrier is expected to be the largest one.

Next, we focused on the geometric parameters of these reactions. In the addition reactions, the •OH radical approaches the C atom perpendicular to the aromatic ring, thus resulting in similar O_{OH}–C distances in all of the characterized transition states, within the range 2.0–2.1 Å, with the exception of the attack on the C8 atom, which shows the longest distance in the transition state (2.125 Å) and the shortest in the intermediate (1.405 Å). This result is in agreement with calculated smaller barriers and the greater stability of the intermediate radical. In the abstraction reaction, the most favored processes (abstraction from the N7 and C10 atoms) show the longest distances between the O atom of the hydroxyl radical and the abstracted H atom and the shortest distances between the atom on the aromatic ring and the abstracted atom. These distances show that, in these cases, the TSs

Table 6. Computed enthalpy values (in kcal mol^{-1}) at dielectric constants of 4 and 80 (in aqueous solution) at the transition states and radical intermediates for the attack of the first •OH radical onto tryptophan, considering two reaction mechanisms, that is, addition and abstraction. The C–O distance (addition) and the C–H and O–H distances (abstraction) are also shown (in Å). The spin densities on the radical O atoms (ρ_s^O) and target C atoms (ρ_s^C) are also presented, as well as the data of one of the reactant complexes.

Trp–•OH complex

	r_{CO}	ΔH_4	ΔH_{aq}	ρ_s^O	ρ_s^C
	2.554	−0.4	0.7	0.91	0.02

OH addition

	r_{CO}^{TS}	ΔH_4^{TS}	ΔH_{aq}^{TS}	ρ_s^O	ρ_s^C	r_{CO}^{Int}	ΔH_4^{Int}	ΔH_{aq}^{Int}	ρ_s^O	ρ_s^C
C2	2.107	0.1	2.0	0.69	−0.12	1.431	−24.4	−21.2	0.00	−0.15
C3	1.975	0.7	1.2	0.62	−0.11	1.429	−15.3	−14.8	0.01	−0.13
C4	2.002	−0.4	0.0	0.64	−0.14	1.427	−17.7	−17.4	0.02	−0.14
C5	2.043	−0.8	−0.1	0.67	−0.11	1.423	−19.8	−19.0	0.02	−0.16
C8	2.125	−5.7	−4.8	0.66	−0.08	1.405	−28.6	−27.4	0.00	−0.01

H abstraction

	r_{CH}^{TS}	r_{OH}^{TS}	ΔH_4^{TS}	ΔH_{aq}^{TS}	ρ_s^O	ρ_s^C	ΔH_4^{Int}	ΔH_{aq}^{Int}
C2	1.209	1.296	1.7	4.4	0.60	0.37	−4.4	−4.2
C3	1.238	1.234	4.7	5.3	0.58	0.41	−3.1	−3.4
C4	1.239	1.231	4.9	5.3	0.59	0.44	−3.3	−3.8
C5	1.243	1.232	5.8	7.0	0.56	0.36	−2.1	−2.2
N7	1.071	1.416	2.2	5.0	0.57	0.24(N)[a]	−24.5	−24.6
C8							3.3	3.1
C10	1.145	1.530	−1.6	0.1	0.78	0.25	−28.7	−27.7

[a] (N)=spin density at N7

occur at a much earlier stage and, therefore, they agree with the smaller calculated barriers for these processes.

We also analyzed the spin density on the O_{OH} atom (ρ_s^O) and on the target C (or N) atom (ρ_s^C). In the addition reactions, the trend was analogous for all aromatic carbon atoms and similar to the observed trends with phenylalanine and tyrosine. Thus, in the infinitely separated reactants, the radical character is fully localized on the O atom of the hydroxyl radical; in the TS structures, ρ_s^O decreases to about 0.65 and part of the radical character has begun to be delocalized over the aromatic rings, whereas, in the adducts, it is fully delocalized over the aromatic ring. On the other hand, in the transition states of the H-abstraction reactions, the radical character is not delocalized over the ring and, instead, is completely localized on the O_{OH} atom and the attacked ring atom. The exception is with the attack on the N atom, where about 20% of the radical character is delocalized over the other ring atoms. The stability that is gained by this delocalization over the remaining ring atoms explains the calculated low enthalpic data. Finally, the radical character on the O_{OH} atom grows to 78% during the attack on the C10 atom, thus indicating that the radical character is transferred less well onto the C10 atom, which is in agreement with the earlier TS observed for this reaction pathway. Recall that, for other aromatic amino acid side chains, similar behavior at the C_β atom was observed.

Attack of a second ·OH radical. As with the other aromatic amino acids, the oxidation of the side-chain atoms with a H atom have been considered, including the aliphatic C10 atom. As in phenylalanine and tyrosine, the product that is formed by H abstraction from the C_α to form a double bond between itself and C_β has also been characterized. The reaction enthalpies of all of the characterized products are listed in Table 7.

Table 7. Computed enthalpy values (in kcal mol^{-1}) at dielectric constants of 4 and 80 (in aqueous solution) calculated with respect to the initial reactants and products that are formed by the attack of a second hydroxyl radical onto tryptophan.

	ΔH_4^{298}	ΔH_{aq}^{298}
$Prod_{Trp}^{C2}$	−116.2	−114.4
$Prod_{Trp}^{C3}$	−113.9	−113.7
$Prod_{Trp}^{C4}$	−114.6	−114.6
$Prod_{Trp}^{C5}$	−114.6	−114.0
$Prod_{Trp}^{N7}$	−74.7	−71.4
$Prod_{Trp}^{C8}$	−123.5	−118.2
$Prod_{Trp}^{C10}$	−111.6	−109.3
$Prod_{Trp}^{10\alpha}$	−104.6	−105.6

The ΔH^{298} values of the oxidized products that are formed when the second radical attacks the adduct radicals that are formed in the six-membered aromatic rings are very similar, with values of about −114 kcal mol^{-1}. These values are very close to the computed enthalpies for the attack on the phenylalanine or tyrosine aromatic rings. Interestingly, the attack at the C8 atom in the five-membered ring affords the most stable product, with ΔH_4^{298} and ΔH_{aq}^{298} values of −123.5 and −118.2 kcal mol^{-1}.

Even though Int_{Trp}^{N7ab} is the most stable adduct that is formed by the attack of the first ·OH radical on the bicyclic group, $Prod_{Trp}^{N7}$ is about 35 kcal mol^{-1} less stable. Similarly, the two products that can be formed from the intermediate that is formed by H abstraction from the aliphatic C10 atom, $Prod_{Trp}^{C10}$ and $Prod_{Trp}^{10\alpha}$ are 10 kcal mol^{-1} less stable than $Prod_{Trp}^{C8}$.

4. Discussion

It is well-known that the side chain of aromatic amino acids are the target of hydroxyl radicals, to form a variety of products (Figure 1 A). However, kinetics and thermodynamics data regarding all of the possible reaction pathways are necessary to gain a better understanding of the process.

The data presented in this work indicate that the reaction thermodynamics are the main driving force and that they prevail over the reaction kinetics. In general, the computed enthalpy barriers are low (the highest ΔH_{aq}^{298} value is 7.0 kcal mol^{-1}) and the difference between the energy barriers of the various characterized reaction pathways is small, in most of the cases within the uncertainty of the method. On the other hand, a larger difference is found between the relative enthalpies of the radical intermediates and the characterized products for the same reaction mechanisms. Therefore, the thermodynamics data may help to shed some light on the preferential targets and pathways that are followed by the radical when it attacks an aromatic amino acid.

In this work, we have considered that the oxidation of any of the atoms in the aromatic amino acid involves the sequential attack of two ·OH radicals and that the reaction proceeds through a radical intermediate. This attack may take place through the addition of a radical or through the abstraction of a hydrogen atom from the amino acid. The thermodynamics data for all of the possible reaction pathways are analogous for the three aromatic amino acids considered. For phenylalanine and tyrosine, the radical intermediates that are formed after the addition of the radical onto any of aromatic positions are roughly 12 kcal mol^{-1} more stable than the intermediates that are formed after hydrogen abstraction. Therefore, these data predict that the first radical attack is an addition to form the radical intermediate and that the second radical abstracts a hydrogen atom from the C atom to form the oxidized product.

This reaction pathway was consistent for all of the aromatic C atoms of Phe and Tyr. However, the most stable radical intermediates that were characterized for these two amino acids did not correspond to addition onto any of these atoms. Instead, the abstraction from the aliphatic C_β atom (C7 atom) produces an intermediate that is about 11 kcal mol^{-1} more stable than the addition intermediates. The computed spin densities indicate that this difference may be due to the fact that, when the radical is added to

any of the aromatic C atoms, the aromaticity of the ring is broken, whereas, when the attack occurs on the aliphatic moiety, the aromaticity is maintained. In addition, the radical character is even more stabilized by its delocalization over the aromatic ring. However, when the second radical eliminates the hydrogen atom from the intermediate radical adduct, the aromaticity in the structure is recovered. As a consequence, oxidation at any of the aromatic ring positions lead to products that are about 5 kcal mol^{-1} more stable than the oxidation of the aliphatic C carbon. These results are in agreement with the experimentally characterized oxidized products for Phe and Tyr.[8]

The presence of an indole group in tryptophan makes the reaction of hydroxyl radicals with this amino acid side chain more complex. One the one hand, the successive attack of two •OH radicals on the benzene group shows enthalpy values that are similar to the reaction with phenylalanine. As with this amino acid, even though H abstraction from the aliphatic C10 atom produces a more stable intermediate, the products that are formed from this intermediate are less favored. Consequently, the calculations predict that the reaction involves the initial addition of the •OH radical to form the adduct, followed by H abstraction. On the other hand, tryptophan contains two additional atoms in the pyrrole ring that are open to radical attack, that is, atoms N7 and C8. The calculations demonstrate that the addition at the C8 atom and abstraction from the N7 atom produce intermediates with very favorable ΔH^{298}_{aq} values, that is, roughly 10 kcal mol^{-1} more stable than those that are formed by the addition on the six-membered ring C atoms. Therefore, these enthalpy values are comparable to those that are formed after hydrogen abstraction from the aliphatic C10 atom, but, unlike this reaction pathway, hydrogen abstraction from the C8 atom produces the most stable product, with a ΔH^{298}_{aq} value of −118.2 kcal mol^{-1}. Therefore, these results indicate that the C8 atom is the most preferred position for the attack of the radicals in tryptophan (the entire reaction pathway is shown in Figure 4) and is more favorable than the attack on phenylalanine or tyrosine.

Experimentally, it has been determined that the radicals can attack any of the positions on the phenylalanine ring,[8] in agreement with our results. Nevertheless, the attack on Tyr produces DOPA, which implies that the radical attacks Tyr at the *meta* positions. However, the computed enthalpies show similar values for the attack on any ring positions, with attack at the *ortho* positions slightly more favorable than at the *meta* positions. Moreover, even though the data indicate that the bi-tyrosine species are thermodynamically less favorable than the oxidation of the ring, these species have been experimentally characterized.[18] All of these data may suggest that, in these reaction pathways, other factors, such as steric effects, the accessibility of the radical to the amino acid side chain positions, and the concentration of the radical, predominate over thermodynamics. At this point, it is worth noting that our calculations were performed on an isolated model that included a single amino acid side chain. This model is suitable for investigating the intrinsic chemistry that governs the reaction, but does not include the influence of a large molecule, such as a protein. We expect that the access of a radical to the target amino acid is highly influenced by the bulk of the protein, which may explain the preference for the radical attack at the *meta* positions of tyrosine to form DOPA, because the *ortho* positions are more hindered by the protein backbone. In this vein, we must bear in mind that the experiments performed by Stadtman[10] indicate that the bulkier the amino acid, the further from the core of the amino acid the radical attacks. Thus, the backbone is the target of the attack with small amino acids, whereas, in larger residues, the reaction occurs on the side chain. On the other hand, bi-tyrosine species can be produced when the radical concentration is sufficient to form the radical intermediates but is insufficient to promote

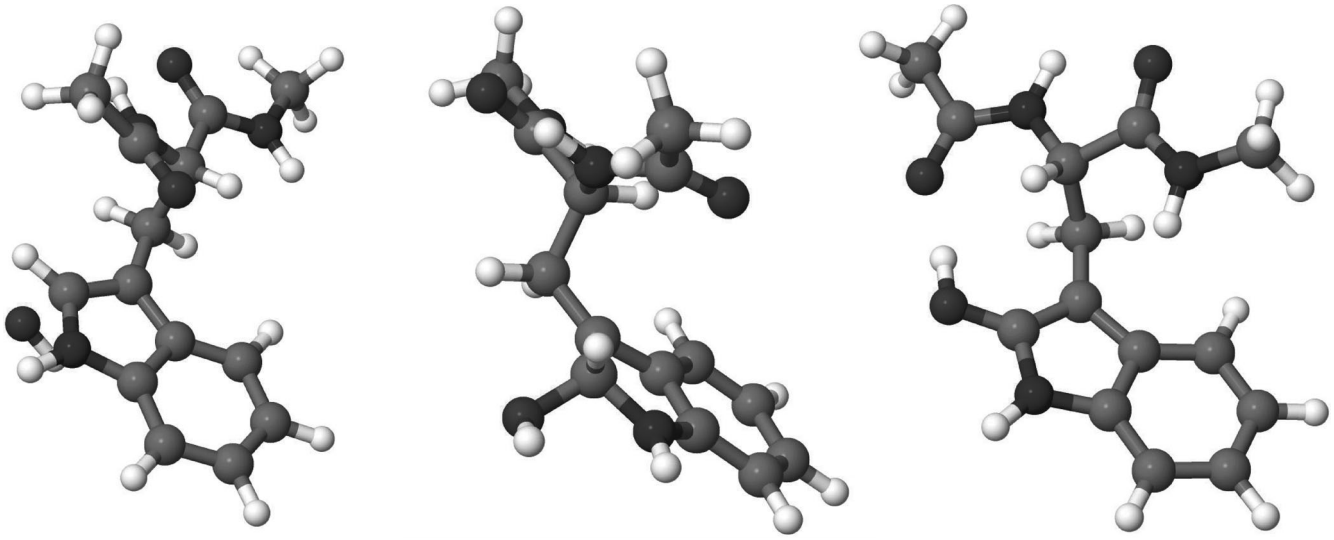

Figure 4. Stationary points (Transition State (TS), left; Intermediate (Int), center; Product (Prod), right) along the most favorable reaction pathway, that is, oxidation at the C8 atom of tryptophan.

an immediate attack of a second radical onto the same side chain to produce the oxidation. In this way, the lifetime of these intermediates is long enough to allow for the formation of the bi-tyrosine species.

Moreover, the ΔH_4^{298} values of all of the characterized products are, in general, 2–3 kcal mol^{-1} lower than their corresponding ΔH_{aq}^{298} values. Interestingly the most stable product (oxidation at the C8 atom of tryptophan) shows the largest difference, with the ΔH_4^{298} value 5 kcal mol^{-1} more stable than the corresponding ΔH_{aq}^{298} value. This trend indicates that the radical attack can be thermodynamically favored in apolar areas of a protein, that is, in buried regions.

Conclusion

The sequential attack of two $^{\bullet}$OH radicals onto three aromatic amino acids, that is, phenylalanine, tyrosine, and tryptophan, have been investigated by using DFT calculations. The low computed enthalpy values confirm that the side chains on the three aromatic amino acids can be the target of hydroxyl radicals. These results indicate that thermodynamics governs the kinetics in these reactions, although other factors, such as radical concentration and steric effects, may also be relevant to this mechanism. Herein, all of the possible attacks of the $^{\bullet}$OH radical onto the aromatic amino acid have been characterized, either by considering the addition of the radical onto the amino acid side chain or hydrogen abstraction. For the three amino acids, the reaction proceeds through a two-step mechanism, in which the first $^{\bullet}$OH radical is added onto the amino acid and the second $^{\bullet}$OH radical abstracts a hydrogen atom to form the oxidized product. The oxidation of the phenylalanine and tyrosine rings, as well the six-membered ring of tryptophan, present very similar enthalpy values. Nevertheless, the most favorable product corresponds to oxidation at the C8 atom of tryptophan, which is located in the five-membered ring of this amino acid. Therefore, this atom is predicted to be the weakest position for radical attack in the three aromatic amino acids that were studied.

Acknowledgements

This research was funded by Eusko Jaurlaritza (the Basque Government, GIC 07/85 IT-330-07) and the Spanish Ministerio de Ciencia e Inovacion (CTQ2011-27374). The SGI/IZO-SGIker UPV/EHU is acknowledged for computational resources. J.M.M. would like to thank the Spanish Ministry of Science and Innovation for funding through a Ramon y Cajal fellowship (RYC 2008-03216).

[1] M. F. Beal, *Free Radical Biol. Med.* **2002**, *32*, 797–803.
[2] K. J. A. Davies, *J. Biol. Chem.* **1987**, *262*, 9895–9901.
[3] B. Halliwell, J. M. C. Gutteridge, *Free Radicals in Biology and Medicine*, Vol. 10, Oxford University Press, Oxford, **1999**.
[4] Y. Zhou, S. Richardson, M. J. Mombourquette, J. A. Weil, *Neurosci. Lett.* **1995**, *195*, 89–92.
[5] D. J. Bonda, X. Wang, G. Perry, A. Nunomura, M. Tabaton, X. Zhu, M. A. Smith, *Neuropharmacology* **2010**, *59*, 290–294.
[6] M. A. Smith, G. Perry, P. L. Richey, I. M. Sayre, V. E. Anderson, M. F. Beal, N. Kowall, *Nature* **1996**, *382*, 120–121.
[7] R. T. Dean, S. L. Fu, R. Stocker, M. J. Davies, *Biochem. J.* **1997**, *324*, 1–18.
[8] E. R. Stadtman, R. L. Levine, *Amino Acids* **2003**, *25*, 207–218.
[9] V. I. Lushchak, *Biochem.* **2007**, *72*, 809–827.
[10] E. R. Stadtman, *Annu. Rev. Biochem.* **1993**, *62*, 797–821.
[11] Z. Maskos, J. D. Rush, W. H. Koppenol, *Arch. Biochem. Biophys.* **1992**, *296*, 521–529.
[12] G. A. Molnár, Z. Wagner, L. Marko, T. Koszegi, M. Mohas, B. Kocsis, Z. Matus, L. Wagner, M. Tamasko, I. Mazak, B. Laczy, J. Nagy, I. Wittmann, *Kidney Int.* **2005**, *68*, 2281–2287.
[13] C. E. Humphrey, M. Furegati, K. Laumen, L. La Vecchia, T. Leutert, J. Constanze, D. Muller-Hartwieg, M. Vogtle, *Org. Process Res. Dev.* **2007**, *11*, 1069–1075.
[14] S. Li, M. Fu, S. F. Habicht, G. O. Pates, J. J. Nash, H. I. Kenttmaa, *J. Org. Chem.* **2009**, *74*, 7724–7732.
[15] H. C. Yeh, G. J. Gerfen, J. S. Wang, A. L. Tsai, L. H. Wang, *Biochemistry* **2009**, *48*, 917–928.
[16] J. Stubbe, W. A. van der Donk, *Chem. Rev.* **1998**, *98*, 705–762.
[17] M. Asanuma, I. Miyazaki, N. Ogawa, *Neurotoxic. Res.* **2003**, *5*, 165–176.
[18] C. Giulivi, N. J. Traaseth, K. J. Davies, *Amino acids* **2003**, *25*, 227–232.
[19] J. W. Heinecke, W. Li, G. A. Francis, J. A. Goldstein, *J. Clin. Invest.* **1993**, *91*, 2866–2872.
[20] Z. Maskos, J. D. Rush, W. H. Koppenol, *Arch. Biochem. Biophys.* **1992**, *296*, 514–520.
[21] T. Todorovski, M. Fedorova, R. Hoffmann, *J. Mass Spectrom.* **2011**, *46*, 1030–1038.
[22] X. Chen, L. Zhang, L. Zhang, J. Wang, H. Liu, Y. Bu, *J. Phys. Chem. B* **2009**, *113*, 16681–16688.
[23] M. Faraggi, M. R. DeFelippis, M. H. Klapper, *J. Am. Chem. Soc.* **1989**, *111*, 5141–5145.
[24] J. M. Matxain, M. Ristila, Å. Strid, L. A. Eriksson, *Chem. Eur. J.* **2007**, *13*, 4636–4642.
[25] J. Mujika, J. M. Matxain, *J. Mol. Model.*, DOI: 10.1007s00894–012–1465–1465.
[26] M. C. Owen, M. Szori, I. G. Csizmadia, B. Viskolcz, *J. Phys. Chem. B* **2012**, *116*, 1143–1154.
[27] J. M. Matxain, D. Padro, M. Ristila, A. Strid, L. A. Eriksson, *J. Phys. Chem. B* **2009**, *113*, 9629–9632.
[28] A. Pérez-González, A. Galano, *J. Phys. Chem. B* **2011**, *115*, 1306–1314.
[29] A. Galano, *Theor. Chem. Acc.* **2011**, *130*, 51–60.
[30] A. Galano, J. R. Alvarez-Idaboy, M. Francisco-Márquez, M. E. Medina, *Theor. Chem. Acc.* **2012**, *131*, 1173–1184.
[31] J. R. León-Carmona, A. Galano, *J. Phys. Chem. B* **2011**, *115*, 4538–4546.
[32] H.-Y. Zhang, L.-F. Wang, *J. Biomol. Struct. Dyn.* **2005**, *22*, 483–486.
[33] Gaussian 09, Revision A.1, M. J. Frisch, G. W. Trucks, H. B. Schlegel, G. E. Scuseria, M. A. Robb, J. R. Cheeseman, G. Scalmani, V. Barone, B. Mennucci, G. A. Petersson, H. Nakatsuji, M. Caricato, X. Li, H. P. Hratchian, A. F. Izmaylov, J. Bloino, G. Zheng, J. L. Sonnenberg, M. Hada, M. Ehara, K. Toyota, R. Fukuda, J. Hasegawa, M. Ishida, T. Nakajima, Y. Honda, O. Kitao, H. Nakai, T. Vreven, J. A. Montgomery, Jr., J. E. Peralta, F. Ogliaro, M. Bearpark, J. J. Heyd, E. Brothers, K. N. Kudin, V. N. Staroverov, R. Kobayashi, J. Normand, K. Raghavachari, A. Rendell, J. C. Burant, S. S. Iyengar, J. Tomasi, M. Cossi, N. Rega, J. M. Millam, M. Klene, J. E. Knox, J. B. Cross, V. Bakken, C. Adamo, J. Jaramillo, R. Gomperts, R. E. Stratmann, O. Yazyev, A. J. Austin, R. Cammi, C. Pomelli, J. W. Ochterski, R. L. Martin, K. Morokuma, V. G. Zakrzewski, G. A. Voth, P. Salvador, J. J. Dannenberg, S. Dapprich, A. D. Daniels, Ö. Farkas, J. B. Foresman, J. V. Ortiz, J. Cioslowski, D. J. Fox, Gaussian, Inc., Wallingford CT, **2009**.

[34] Y. Zhao, B. J. Lynch, D. G. Truhlar, *J. Phys. Chem. A* **2004**, *108*, 2715–2719.
[35] Y. Zhao, B. J. Lynch, D. G. Truhlar, *J. Phys. Chem. A* **2004**, *108*, 4786–4791.
[36] Y. Zhao, J. Pu, B. J. Lynch, D. G. Truhlar, *Phys. Chem. Chem. Phys.* **2004**, *6*, 673–676.
[37] Y. Zhao, D. G. Truhlar, *J. Phys. Chem. A* **2004**, *108*, 6908–6918.
[38] P. Hohenberg, W. Kohn, *Phys. Rev.* **1964**, *136*, B864.
[39] W. Kohn, L. J. Sham, *Phys. Rev.* **1965**, *140*, A1133.
[40] B. Mennucci, J. Tomasi, *J. Chem. Phys.* **1997**, *106*, 5151–5158.
[41] J. Tomasi, B. Mennucci, E. Cances, *J. Mol. Struct.: THEOCHEM* **1999**, *464*, 211–226.
[42] I. Tejero, A. Gonzalez-Lafont, J. M. Lluck, L. A. Eriksson, *Chem. Phys. Lett.* **2004**, *398*, 336–342.
[43] J. M. Matxain, M. Ristila, A. Strid, L. A. Eriksson, *J. Phys. Chem. A* **2006**, *110*, 13068–13072.

Received: October 29, 2012
Revised: January 15, 2013
Published online: March 27, 2013

